HHS Public Access

Author manuscript

FASEB J. Author manuscript; available in PMC 2022 August 01.

Published in final edited form as:

FASEB J. 2021 August ; 35(8): e21772. doi:10.1096/fj.202100021R.

Ablation of Sam68 in adult mice increases thermogenesis and energy expenditure

Aijun Qiao[1,*], **Wenxia Ma**[1], **Jianxin Deng**[1], **Junlan Zhou**[2], **Chaoshan Han**[1], **Eric Zhang**[1], **Chan Boriboun**[1], **Shiyue Xu**[1], **Chunxiang Zhang**[1], **Chunfa Jie**[3], **Jeong-a Kim**[4], **Kirk Habegger**[4], **Hongyu Qiu**[5], **Ting C Zhao**[6], **Jianyi Zhang**[1], **Gangjian Qin**[1,2,*]

[1]Department of Biomedical Engineering, University of Alabama at Birmingham, School of Medicine and School of Engineering, Birmingham, AL 35294, USA

[2]Feinberg Cardiovascular Research Institute, Northwestern University Feinberg School of Medicine, Chicago, IL 60611, USA

[3]Department of Biochemistry and Nutrition, Des Moines University Medicine and Health Sciences, Des Moines, IA 50312, USA

[4]Department of Medicine - Endocrinology, Diabetes & Metabolism, Comprehensive Diabetes Center, University of Alabama at Birmingham, School of Medicine, Birmingham, AL 35294, USA

[5]Center of Molecular and Translational Medicine, Institution of Biomedical Science, Georgia State University, Atlanta, GA 30303, USA

[6]Department of Surgery, Boston University Medical School, Roger Williams Medical Center, Providence, RI 02908, USA

Abstract

Genetic deletion of Sam68, a pleiotropic adaptor protein prevents high-fat-diet–induced weight gain and insulin resistance. To clarify the role of Sam68 in energy metabolism in the adult stage, we generated an inducible Sam68 knockout mice. Knockout of Sam68 was induced at the age of 7-10 weeks, and then we examined the metabolic profiles of the mice. Sam68 knockout mice gained less body weight over time and at 34 or 36 weeks old, had smaller fat mass without changes in food intake and absorption efficiency. Deletion of Sam68 in mice elevated thermogenesis, increased energy expenditure, and attenuated core-temperature drop during acute cold exposure. Furthermore, we examined younger Sam68 knockout mice at 11 weeks old before their body weights deviate, and confirmed increased energy expenditure and thermogenic gene

[*]Correspondence should be addressed to: Gangjian Qin, MD, Professor, Department of Biomedical Engineering, School of Medicine & School of Engineering, University of Alabama at Birmingham, 1720 2nd Ave S., VH G094N, Birmingham, AL 35294, USA, Tel: (205) 934-6690; Fax: (205) 934-9101, gqin@uab.edu; Aijun Qiao, PhD, Assistant Professor, Department of Biomedical Engineering, School of Medicine & School of Engineering, University of Alabama at Birmingham, 1720 2nd Ave S., VH G094R, Birmingham, AL 35294, USA, Tel: (205) 934-5928; Fax: (205) 934-9101, aqiao@uab.edu.

Author Contributions

A.Q. and G.Q. conceptualized the study, designed the experiments, interpreted data, and wrote the manuscript. A.Q. performed most of the experiments and statistical analyses. W.M., J.D., J.Z., C.H., E.Z., C.B., and S.X. performed experiments and analyzed data. C.Z., J.F., J.K., K.H., H.Q., T.C.Z. and J.Z. made intellectual contributions and assisted in data interpretation and manuscript editing.

Conflict of Interest Statement

The authors have stated explicitly that there are no conflicts of interest in connection with this article.

program. Thus, Sam68 is essential for the control of adipose thermogenesis and energy homeostasis in the adult.

Keywords

Sam68; Obesity; Adipose; Thermogenesis; Energy metabolism; UCP1; Browning; Adipocytes

Introduction

The adipose tissues, including white adipose tissue (WAT), brown adipose tissue (BAT), and beige/brite adipose tissue, play a major role in energy homeostasis (1). In rodents, WAT and BAT represent 95% and 1-2% of the total body fat mass, respectively, and beige/brite adipose is difficult to quantitate because beige/brite adipocytes are interspersed within WAT and capable of transforming into brown-like adipocytes following cold exposure or adrenergic stimulation, a process termed WAT "browning" (1). Characteristically, white adipocytes carry a unilocular large lipid droplet and primarily store energy, whereas brown and beige adipocytes contain multilocular small droplets and abundant mitochondria and express thermogenic genes including UCP1 (uncoupling protein 1), which mediates uncoupling of oxidative phosphorylation through proton leakage across the inner mitochondrial membrane to generate heat, and PGC-1α (peroxisome proliferator-activated receptor gamma coactivator 1-alpha), Cox8b (cytochrome c oxidase subunit 8B), Cidea (cell death-inducing DNA fragmentation factor-like effector A) and Elovl3 (elongation of very long chain fatty acids protein 3), which regulate mitochondrial biogenesis, oxidative phosphorylation, and lipolysis, respectively (2, 3). Brown and beige adipocytes have similar morphology and thermogenic capacity and respond similarly to neuroendocrine signals (4), but differ in transcriptional signature and thermogenic plasticity; while brown adipocytes constitutively express high levels of thermogenic genes and their thermogenic activity can be further augmented, beige adipocytes express low levels of thermogenic genes in the basal state and their thermogenic program can be robustly induced by external stimuli (5, 6), during which the zinc-finger transcriptional factor PR domain containing 16 (Prdm16) acts as a powerful driver of beige cell fate (7).

An important function of thermogenesis is maintaining body temperature during cold exposure; for example, mice housed at room temperature (20-22°C) are under cold stimulation and must therefore expend extra energy to defend their body temperature (8). Traditionally, the presence of BAT was thought to be relevant only in rodents and human infants. However, over the past decade, it has been unequivocally demonstrated that human adults possess active brown and beige adipocytes (9, 10). It has now become clear that brown and beige adipocytes are not simply heat-generating cells and they regulate energy metabolism through sophisticated mechanisms (6, 11). In rodents, BAT and WAT "browning" can facilitate weight loss and improve systemic metabolism, including glucose tolerance and insulin sensitivity in obese animals (12, 13). In humans, both retrospective and prospective studies demonstrate close associations of BAT activity with energy metabolic states, an increased activity correlated with leanness and beneficial glucose and lipid profiles (14, 15) and a decreased activity associated with ageing, obesity and metabolic diseases (13,

16, 17). Therefore, enhancing BAT activity and WAT "browning" has been considered a potential therapeutic strategy for combat of obesity and its associated metabolic disorders (8, 13), although debate remains regarding the extent to which they contribute to energy expenditure and weight loss, optimal methods to maximize their recruitment and activity, and potential effects of counter-regulatory mechanisms (18, 19).

Src-associated-in-mitosis-of-68kDa (Sam68; also known as KH-domain–containing, RNA-binding, signal-transduction–associated 1 [KHDRBS1]) is a member of the signal-transducer-and-activator-of-RNA (STAR) family of RNA-binding proteins (20, 21) and involved in numerous cellular functions, including RNA processing (22, 23), kinase and growth-factor signaling (24, 25), transcription (26, 27), cell-cycle regulation, and apoptosis (28, 29). The range of its activities is reflected in the diverse phenotypes observed in Sam68 knockout (*Sam68*$^{-/-}$) mice, including an increased neonatal lethality and defects in spermatogenesis and age-associated bone decalcification (30-32). Strikingly, their body weight and adiposity were reduced and the mice were resistance to high-fat-diet induced obesity and diabetes (33, 34). We have previously reported an increased thermogenesis in *Sam68*$^{-/-}$ mice (33). However, *Sam68*$^{-/-}$ mice also display an impaired adipose differentiation (34) and increased neonatal lethality (32).Thus, it remains unknown if the enhanced thermogenic program in Sam68$^{-/-}$ mice is the result of skewed adipose development or indeed an altered adipose metabolism.

In this study, we generated an inducible Sam68 knockout mouse line, and revealed that ablation of Sam68 in the adult stage leads to reduced body weight, increased adipose thermogenesis and energy expenditure. These results suggest that Sam68 is an essential regulator of adipose metabolism and systemic energy homeostasis.

Materials and Methods

Mice

All animal studies in this report were approved by the Institutional Animal Care and Use Committees (IACUC) of Northwestern University and the University of Alabama at Birmingham and comply with relevant ethical regulations, including the National Institutes of Health (NIH) "Guide for the Care and Use of Laboratory Animals". Experiments were conducted in C57BL/6J male mice that were fed at libitum and maintained under a 12:12-h light:dark cycle. Sam68$^{f/W}$ mice were generated at the Transgenic and Targeted Mutagenesis Laboratory in the Center for Genetic Medicine at Northwestern University by transfecting C57BL/6N embryonic stem cells with a targeting vector pGK-Sam68$^{floxEx5\text{-}8}$, which was constructed from the pGKneoF2L2DTA plasmid and harbors homologous sequences of the *Sam68* allele and *loxP* sites inserted into introns 4 and 8. After validation with Southern blotting and sequencing of genomic DNAs, the Sam68$^{f/w}$ C57Bl/6N mice were back-crossed to C57BL/6J mice for 10 generations; then Sam68$^{f/f}$ mice, produced by interbreeding Sam68$^{f/w}$ heterozygote mice, were crossed with mice carrying *CAGG-Cre-ER*^{TM} transgene [B6.Cg-Tg (CAG-cre/Esr1*) 5Amc/J], Jax Lab, No. 004682) to generate *CAGG-Cre;Sam68*$^{f/f}$ mice. For induction of Sam68 deletion, seven weeks-old *CAGG-Cre;Sam68*$^{f/f}$ mice were fed a tamoxifen-containing diet (400 mg/kg tamoxifen citrate, 5% sucrose, 95% Teklad Global, 16% Rodent Diet from Harland Teklad [TD130855]) for 3 consecutive

weeks. Subsequently, the mice were returned to a diet of standard mouse chow provided by the UAB Animal Resources Program (ARP) for another 24 or 26 weeks. *Sam68*$^{f/f}$ mice that underwent same treatment were used as controls.

Quantitative magnetic resonance (QMR) analysis of body compositions

Body composition (total body fat and lean tissues) of mice was determined using an EchoMRI™ 3-in-1 QMR machine (Echo Medical Systems, Houston, TX). A system test was performed using a known fat standard prior to the measurements being taken. Mice were weighed and then placed into a clear holding tube capped with a stopper that restricted vertical movement, but allowed constant airflow. The tube was inserted into the machine and the mouse scanned using a primary accumulation of 1 and measuring total body water in addition to fat and lean mass.

Indirect calorimetry analysis

Oxygen consumption (VO2), carbon dioxide production (VCO2), energy expenditure, respiratory exchange ratio (RER), and locomotor activity were acquired using an 8-cage indirect calorimetry system (Labmaster; TSE Systems, Bad Homburg, Germany). Mice were acclimated to the cages for 48 h prior to the measurement period of 48 h. During the entire experiment, mice were individually housed in indirect-calorimetry chambers, fresh air was supplied at 0.55L/min, and oxygen consumption and carbon dioxide production were measured for 1 min every 9 min. Total energy expenditure represented the average hourly energy expenditure over 48 h. Resting energy expenditure was calculated from the average energy expenditure over three nonconsecutive 10-min intervals during which energy expenditure was minimal, with at least 1 h between each period. Locomotor activity was determined with infrared beams for horizontal (x, y) activity.

Bomb calorimetry analysis

Mice were housed in new cages containing minimal bedding for a period of 72 h, following which the mice were transferred to new clean cages. All feces produced during this period were carefully collected from the bedding, weighed, and frozen until the bomb calorimetry measurement. Fecal energy (gross energy [GE] of feces, kilocalories per gram) and the energy density of the diets (GE of food, kilocalories per gram) were measured by bomb calorimetry in the UAB Small Animal Phenotyping Core. Energy content was determined in triplicate with a Parr1261 calorimeter (Parr Instrument Company, Moline, IL). The average energy value was used for each sample and multiplied by the dry weight of sample to get energy in or out. The food absorption efficiency (AE, %) was calculated using the following equation:

$$\mathbf{AE}(\%) = \frac{\left[\mathbf{Dry\ Food\ Intake(g\ in\ 96\ h)} \times \mathbf{GE\ of\ Food}\left(\frac{\mathbf{kcal}}{\mathbf{g}}\right)\right] - \left[\mathbf{Fecal\ Output\ (g\ in\ 96\ h)} \times \mathbf{GE\ of\ Feces}\left(\frac{\mathbf{kcal}}{\mathbf{g}}\right)\right]}{\left[\mathbf{Dry\ Food\ Intake\ (g\ in\ 96\ h)} \times \mathbf{GE\ of\ Food}\left(\frac{\mathbf{kcal}}{\mathbf{g}}\right)\right]}$$

Cold stress and core body-temperature measurements

For cold exposure experiments, mice were placed in a designated cold room (4°C) with free access to food and water. The core body temperature was monitored using a rectal probe (ThermoWorks, ALPINE, UTAH, USA) at 0 (basal), 30 min and 1, 2, 4, and 6 h.

Histology

Hematoxylin and eosin (H&E) staining and immunohistochemistry were performed as we previously described (33). Briefly, ingWAT, epiWAT, and BAT were fixed in 10% neutral buffered formalin, embedded in paraffin, and cut into 7-μm sections. For immunohistochemical staining of UCP1, anti-UCP1 antibody (1:100, ab10983, Abcam, Cambridge, MA) was used, and nuclei were counterstained with hematoxylin. The sections were photographed under a light microscope (Olympus IX83 Microscope, Olympus America Inc.).

Western blotting

For protein extraction, $1x10^7$ cells or 100 mg of frozen tissue were homogenized in 1 mL RIPA lysis buffer (50 mM Tris-HCl pH 8.0, 1 mM EDTA, 1% Triton X-100, 0.1% SDS, 150 mM NaCl), which contains protease-inhibitor (Sigma, 4693132001) and phosphatase-inhibitor (Sigma, 4906837001) cocktails. Samples were incubated with agitation for 30 min at 4°C and centrifuged at 13000 rpm for 10 min at 4°C; then, supernatant was collected, and the protein concentration was determined via bicinchoninic acid (BCA) assay (Pierce). For immunoblotting, proteins in the supernatant were denatured by heating at 95°C for 10 min, separated by SDS-PAGE, then transferred onto a polyvinylidene difluoride (PVDF) membrane (Bio-Rad). The membrane was incubated in 5% non-fat milk blocking buffer (tris-buffered saline [TBS]) for 1 h, incubated with primary antibody in TBS-containing 3% bovine serum albumin (BSA) overnight at 4°C, washed 3 times with TBST (0.5 % Tween 20), incubated with secondary antibody, washed with TBST, then developed with Enhanced Chemiluminescence Detection Reagents (ECL, Thermo Fisher). Protein signals were imaged with a Bio-Rad ChemiDoc System. All antibodies used are reported in Supplementary Table S1. The intensities of protein bands were quantified using NIH Image J software and normalized to the values of β-tubulin.

Quantitative real-time polymerase chain reaction (qRT-PCR)

Total RNA was isolated with TRIzol Reagent and reverse transcribed into cDNA with Reverse Transcription Reagents (Applied Biosystems); then, tissue mRNA levels were determined by qPCR (ABI3000; Applied Biosystems) with SYBR Green Real-Time PCR Master Mix (Applied Biosystems). Duplicate reactions were performed for each sample, and the relative mRNA expression level for each gene was calculated via the 2(-ΔΔCt) method and normalized to β-actin. Primers are reported in Supplementary Table S2.

Statistical analysis

Data are presented as mean ± standard error of the mean (s.e.m.). Statistical significance was evaluated via the unpaired two-tailed Student's *t* test for comparisons between two groups (GraphPad Prism8 Software), via analysis of variance (ANOVA) for comparisons among 3

or more groups with one (one-way) or two (two-way) independent variables (GraphPad Prism8 Software), or via analysis of covariance (ANCOVA) for comparisons where the effects of uncontrolled independent variables (covariates) are taken into account (IBM® SPSS Statistics 27 Standard Software). A p-value of less than 0.05 was considered significant.

Results

Ablation of Sam68 in adult mice leads to body weight reduction

Sam68-floxed (Sam68$^{f/w}$) mice were generated via homologous recombination, back-crossed onto C57BL/6J background, then serially bred with *CAGG-Cre-ER^{TM}* mice to produce mice carrying a tamoxifen-inducible Sam68 knockout mutation (*CAGG-Cre;Sam68$^{f/f}$*) (Figure 1A). At 7 weeks old, *CAGG-Cre;Sam68$^{f/f}$* mice and *Sam68$^{f/f}$* littermates were fed tamoxifen-containing chow for 3 consecutive weeks, then subsets of animals in both groups were sacrificed to confirm that Sam68 protein expression was lost or dramatically reduced in multiple tissues (i.e. liver, spleen, epiWAT, BAT, ingWAT, skeletal muscle, heart, lung, and kidney) of *CAGG-Cre;Sam68$^{f/f}$* (*Sam68^{iKO}*) mice (Figure 1B). The remaining mice were continually monitored for changes in body weight for another 24 or 26 weeks, then evaluated for energy metabolism and gene expressions. We found that tamoxifen treatment induced a transient reduction in the body weight of both groups to similar degree (Figure 1C). Thereafter, the curves of body-weight gain diverged progressively, and Sam68^{iKO} mice were 19% lighter than *Sam68$^{f/f}$* littermates at 34 weeks old (24 weeks after completion of tamoxifen treatment) (Figure 1C). Thus, Sam68 plays an important role in maintaining the body weight in adult mice.

Ablation of Sam68 in adult mice leads to decreased adiposity

To gain a detailed understanding of the body-weight difference between *Sam68^{iKO}* and *Sam68$^{f/f}$* mice (Figure 2A), we analyzed their body compositions. Sam68^{iKO} mice displayed significantly reduced fat mass (by 40%) and lean mass (by 11%), as compared to Sam68$^{f/f}$ littermates (Figure 2B), and the reduction in fat mass was still significant after taking body-weight difference into consideration (Figure 2C). Consistently, both white fat (ingWAT, epiWAT and retroWAT) (Figure 2D) and brown fat (Figure 2E) depots were reduced in *Sam68^{iKO}* mice. The liver weight was also lower in *Sam68^{iKO}* mice (Figure 2F), but the heart weight was similar between the two groups of mice (Figure 2G). Notably, the femur and tibia lengths were similar between *Sam68^{iKO}* and *Sam68$^{f/f}$* mice (Figure 2H-I). Collectively, these results suggest that the reduced body weight in *Sam68^{iKO}* mice was primarily attributable to the reduced fat mass.

Ablation of Sam68 in adult mice enhances energy expenditure

To understand the role of Sam68 in the whole-body energy balance, we performed indirect calorimetry analysis in *Sam68^{iKO}* mice and *Sam68$^{f/f}$* littermates at 34 weeks old. Food intakes (Figure 3A) and food absorption efficiencies (Figure 3B) were similar between the two groups of animals. Remarkably, under both light and dark phases, *Sam68^{iKO}* mice display significantly higher oxygen consumption (Figure 3C). The respiratory exchange ratios (RER) in *Sam68^{iKO}* mice were slightly increased under light phase but significantly

higher in the dark phase than *Sam68*$^{f/f}$ littermates (Figure 3D). Consistently, both total and resting energy expenditures were markedly greater in *Sam68*^{iKO} mice than in *Sam68*$^{f/f}$ littermates (Figure 3E-G), and this was not due to reduced lean mass in *Sam68*^{iKO} mice as ANCOVA indicates that energy expenditure increases were independent of changes in lean mass between the two genotypes (Figure 3F-G). The locomotor activity in *Sam68*^{iKO} mice was slightly increased, but the difference was not significant under both light and dark phases (Figure 3H). Collectively, these results suggest that the reduced body weight in *Sam68*^{iKO} mice is the result of increased energy expenditure.

Ablation of Sam68 in adult mice leads to enhanced thermogenesis in BAT

Consistent with the smaller BAT (Figure 2E), *Sam68*^{iKO} mice have reduced lipid stores in brown adipocytes at room temperature (Figure 4A). Notably, *Sam68*^{iKO} mice express higher levels of UCP1 protein expression in BAT than *Sam68*$^{f/f}$ littermates (Figure 4B-C). Consistently, the elevated UCP1 mRNA level was accompanied by increased expression of multiple key thermogenic genes, including PGC-1α, Cox8b, Cidea, Elovl3, and deiodinase 2 (Dio2), but without a concomitant increase in adipose tissue marker genes, such as fatty acid-binding protein 4 (Fabp4) and peroxisome proliferator-activated receptor gamma (PPARγ) (Figure 4C-D). Consistent with the increased thermogenic program, *Sam68*^{iKO} mice were better protected from core temperature drop during acute cold exposure as compared to *Sam68*$^{f/f}$ littermates (Figure 4E). Thus, deletion of Sam68 in adult mice stimulates UCP1 activation, leading to enhanced thermogenic activity.

Ablation of Sam68 in adult mice leads to enhanced WAT browning

Interestingly, the adipocytes from both ingWAT and epiWAT are smaller in *Sam68*^{iKO} mice than in *Sam68*$^{f/f}$ mice (Figure 5A). Since WAT browning can also enhance energy expenditure and facilitate weight loss, we analyzed UCP1 expression in the ingWAT; UCP1-positive adipocytes were much more abundant in *Sam68*^{iKO} mice than in *Sam68*$^{f/f}$ controls (Figure 5B). The mRNA and protein expression of thermogenic genes (e.g. UCP1, Prdm16) were upregulated in ingWAT, as BAT, but not in epiWAT of *Sam68*^{iKO} mice (Figure 5C-E). Although PGC-1α mRNA expression was not changed, its protein level was much higher in ingWAT of *Sam68*^{iKO} mice than in *Sam68*$^{f/f}$ littermates (Figure 5C-D). These results suggest that ablation of Sam68 in adult mice triggers ingWAT browning.

Ablation of Sam68 in adult mice leads to increased energy expenditure and thermogenic gene expression before their body weights deviate

Sam68^{iKO} mice at 34 or 36 weeks old display reduced body weight and elevated energy expenditure. To verify that the increased energy expenditure in these mice was not cause by altered body weight, we performed indirect calorimetry analysis in younger *Sam68*^{iKO} mice and *Sam68*$^{f/f}$ littermate controls at age of 11 weeks (i.e., one week after completion of tamoxifen treatment) when their body weights were comparable. While food intakes (Figure 6A) were similar between the two groups, *Sam68*^{iKO} mice displayed a significantly higher rate of oxygen consumption than *Sam68*$^{f/f}$ mice under both light and dark phases (Figure 6B). While RER between the two groups were equivalent (Figure 6C), both total and resting energy expenditures were significantly greater in Sam68^{iKO} mice than in Sam68$^{f/f}$ littermates (Figure 6D-E). Similar to the older mice, young Sam68^{iKO} mice exhibits slight

increase in locomotor activity under dark phases (Figure 6F). As expected, the mRNA levels of genes involved in thermogenesis and fatty acid oxidation in BAT (Figure 6G) and ingWAT (Figure 6H) were also significantly elevated in young *Sam68*^{iKO} mice compared to *Sam68*$^{f/f}$ controls. Collectively, our data demonstrate that acute deletion of *Sam68* in mice leads to upregulated adipose thermogenesis and energy expenditure.

Discussion

In this study, we demonstrate that ablation of *Sam68* gene in adult mice leads to reduced fat mass and body weight due to elevated energy expenditure from adipose thermogenesis; thus, Sam68 plays an essential role in the control of adipose metabolism and systemic energy homeostasis. The reduced adiposity of *Sam68*$^{-/-}$ mice was linked to a defect in adipose differentiation during development (34). However, in *Sam68*^{iKO} mice with acute ablation of Sam68 at adult stage, we found that the expression of adipocyte marker genes, including PPARγ and Fabp4, are unaltered in all adipose tissues. Strikingly, Prdm16, a powerful driver for brown and beige cell fate (7), is significantly upregulated in ingWAT, and the mRNA and protein levels of multiple thermogenic genes were dramatically increased in both BAT and ingWAT. Since the development of adipose tissue is largely completed at birth and only a small portion of adipocytes are renewed each year in humans (approximately 8–9%) and mice (35, 36), our results suggest that the primary function of Sam68 in adult is to suppress adipose thermogenesis and browning. Notably, the increased thermogenesis in the BAT of *Sam68*^{iKO} mice is characterized by markedly upregulation of Cox8b and Cidea, suggesting that Sam68 may promote thermogenesis through regulating mitochondria and lipolysis (37).

In *Sam68*^{iKO} mice, we also observed a reduced lean mass, but the femur and tibia lengths are unaltered. Thus, the reduced body weight in these mice may involve additional mechanisms, nevertheless appears not due to growth retardation. Likewise, the reduced adiposity in *Sam68*^{iKO} mice is apparently distinct from lipodystrophy, which is associated with metabolic disorders similar to those found in individuals with an excess of adipose tissue (38, 39), whereas *Sam68*$^{-/-}$ mice are characterized with an improved systemic metabolic profile (33, 34).

Adaptive thermogenesis is executed primarily in adipose tissues (8, 40), however can be regulated by various neuroendocrine factors such as sympathetic nervous activity (41, 42). A weakness of our report is yet to pinpoint the precise location where Sam68 exerts these observed effects and whether they are originated within adipose tissues or secondary to altered upstream neuroendocrine signals. Of note, Sam68 is abundantly expressed in tissues (i.e., neurons, liver, muscle and macrophages) known to be involved in the regulation of adipose thermogenesis (4). Further studies to generate multiple tissue-type specific Sam68 knockout mice and characterize their metabolic phenotypes are underway to reveal the relative contributions of diverse tissues.

In conclusion, we present definitive evidence that Sam68 plays an essential role in the control of adipose thermogenesis and energy expenditure in adult mice. Thus, inhibition of Sam68 activity may have beneficial effects for combating obesity and associated metabolic disorders.

Supplementary Material

Refer to Web version on PubMed Central for supplementary material.

Acknowledgements

We thank Dr. Maria S. Johnson and Dr. Timothy R Nagy at the UAB Small Animal Phenotyping Core for the assistance in the bomb calorimetry and indirect calorimetry analyses; the core is supported by the National Institutes of Health Nutrition & Obesity Research Center (P30DK056336), Diabetes Research Center (P30DK079626) and the UAB Nathan Shock Center (P30AG050886A). We thank Dr. Guang Ren (UAB Department of Medicine - Endocrinology) for assistance in cold exposure experiments and Dr. Ying Jiang (UAB Department of Biomedical Engineering) for assistance in data collection during the manuscript revision.

Sources of Funding

This work was supported by the National Institute of Health (R01 Grants# HL138990, HL131110, HL130052, and HL113541 to G.Q.; HL142291 to H.Q & G.Q.; R01DK112934 to K.M.H); American Diabetes Association (Grant# 1-15-BS-148 to G.Q.); American Heart Association (Grant# 19TPA34910227 to G.Q.; 19CDA34630052 to A.Q; 18POST34070088 to S.X; and 18PRE34080358 to E.Z.).

Data Availability

All data are presented in the report. Additional details are available on reasonable request.

Nonstandard Abbreviations

BAT	Brown adipose tissue
Cidea	Cell death-inducing DNA fragmentation factor-like effector A
Cox8b	Cytochrome c oxidase subunit 8B
Dio2	Deiodinase 2
Elovl3	Elongation of very long chain fatty acids protein 3
epiWAT	Epididymal white adipose tissue
Fabp4	Fatty acid-binding protein 4
ingWAT	Inguinal white adipose tissue
PGC-1α	Peroxisome proliferator-activated receptor gamma coactivator 1-alpha
PPARγ	Peroxisome proliferator-activated receptor gamma
Prdm16	PR domain containing 16
QMR	Quantitative magnetic resonance
RER	Respiratory exchange ratios
retroWAT	Retroperitoneal white adipose tissue
Sam68	Src associated in mitosis of 68kDa

UCP1	Uncoupling protein 1
VO2	Oxygen consumption
VCO2	Carbon dioxide production
WAT	White adipose tissue

References

1. Rosen ED, and Spiegelman BM (2014) What we talk about when we talk about fat. Cell 156, 20–44 [PubMed: 24439368]
2. Chouchani ET, Kazak L, and Spiegelman BM (2019) New Advances in Adaptive Thermogenesis: UCP1 and Beyond. Cell metabolism 29, 27–37 [PubMed: 30503034]
3. Ricquier D, and Kader JC (1976) Mitochondrial protein alteration in active brown fat: a soidum dodecyl sulfate-polyacrylamide gel electrophoretic study. Biochemical and biophysical research communications 73, 577–583 [PubMed: 1008874]
4. Wang S, and Yang X (2017) Inter-organ regulation of adipose tissue browning. Cellular and molecular life sciences : CMLS 74, 1765–1776 [PubMed: 27866221]
5. Ikeda K, Maretich P, and Kajimura S (2018) The Common and Distinct Features of Brown and Beige Adipocytes. Trends in endocrinology and metabolism: TEM 29, 191–200 [PubMed: 29366777]
6. Kajimura S, Spiegelman BM, and Seale P (2015) Brown and Beige Fat: Physiological Roles beyond Heat Generation. Cell metabolism 22, 546–559 [PubMed: 26445512]
7. Wang W, Ishibashi J, Trefely S, Shao M, Cowan AJ, Sakers A, Lim HW, O'Connor S, Doan MT, Cohen P, Baur JA, King MT, Veech RL, Won KJ, Rabinowitz JD, Snyder NW, Gupta RK, and Seale P (2019) A PRDM16-Driven Metabolic Signal from Adipocytes Regulates Precursor Cell Fate. Cell metabolism 30, 174–189 e175 [PubMed: 31155495]
8. Harms M, and Seale P (2013) Brown and beige fat: development, function and therapeutic potential. Nature medicine 19, 1252–1263
9. Cypess AM, Lehman S, Williams G, Tal I, Rodman D, Goldfine AB, Kuo FC, Palmer EL, Tseng YH, Doria A, Kolodny GM, and Kahn CR (2009) Identification and importance of brown adipose tissue in adult humans. N Engl J Med 360, 1509–1517 [PubMed: 19357406]
10. Lim J, Park HS, Kim J, Jang YJ, Kim JH, Lee Y, and Heo Y (2020) Depot-specific UCP1 expression in human white adipose tissue and its association with obesity-related markers. Int J Obes (Lond) 44, 697–706 [PubMed: 31965068]
11. Kahn CR, Wang G, and Lee KY (2019) Altered adipose tissue and adipocyte function in the pathogenesis of metabolic syndrome. The Journal of clinical investigation 129, 3990–4000 [PubMed: 31573548]
12. Seale P, Conroe HM, Estall J, Kajimura S, Frontini A, Ishibashi J, Cohen P, Cinti S, and Spiegelman BM (2011) Prdm16 determines the thermogenic program of subcutaneous white adipose tissue in mice. The Journal of clinical investigation 121, 96–105 [PubMed: 21123942]
13. Betz MJ, and Enerback S (2018) Targeting thermogenesis in brown fat and muscle to treat obesity and metabolic disease. Nature reviews. Endocrinology 14, 77–87
14. Iwen KA, Backhaus J, Cassens M, Waltl M, Hedesan OC, Merkel M, Heeren J, Sina C, Rademacher L, Windjager A, Haug AR, Kiefer FW, Lehnert H, and Schmid SM (2017) Cold-Induced Brown Adipose Tissue Activity Alters Plasma Fatty Acids and Improves Glucose Metabolism in Men. J Clin Endocrinol Metab 102, 4226–4234 [PubMed: 28945846]
15. Yoneshiro T, Aita S, Matsushita M, Kameya T, Nakada K, Kawai Y, and Saito M (2011) Brown adipose tissue, whole-body energy expenditure, and thermogenesis in healthy adult men. Obesity (Silver Spring) 19, 13–16 [PubMed: 20448535]
16. van Marken Lichtenbelt WD, Vanhommerig JW, Smulders NM, Drossaerts JM, Kemerink GJ, Bouvy ND, Schrauwen P, and Teule GJ (2009) Cold-activated brown adipose tissue in healthy men. N Engl J Med 360, 1500–1508 [PubMed: 19357405]

17. Darcy J, and Tseng YH (2019) ComBATing aging-does increased brown adipose tissue activity confer longevity? Geroscience 41, 285–296 [PubMed: 31230192]
18. Tam CS, Lecoultre V, and Ravussin E (2012) Brown adipose tissue: mechanisms and potential therapeutic targets. Circulation 125, 2782–2791 [PubMed: 22665886]
19. Trayhurn P (2018) Brown Adipose Tissue-A Therapeutic Target in Obesity? Front Physiol 9, 1672 [PubMed: 30532712]
20. Fumagalli S, Totty NF, Hsuan JJ, and Courtneidge SA (1994) A target for Src in mitosis. Nature 368, 871–874 [PubMed: 7512695]
21. Lukong KE, and Richard S (2003) Sam68, the KH domain-containing superSTAR. Biochim Biophys Acta 1653, 73–86 [PubMed: 14643926]
22. Bielli P, Busa R, Paronetto MP, and Sette C (2011) The RNA-binding protein Sam68 is a multifunctional player in human cancer. Endocr Relat Cancer 18, R91–R102 [PubMed: 21565971]
23. Iijima T, Wu K, Witte H, Hanno-Iijima Y, Glatter T, Richard S, and Scheiffele P (2011) SAM68 regulates neuronal activity-dependent alternative splicing of neurexin-1. Cell 147, 1601–1614 [PubMed: 22196734]
24. Huot ME, Brown CM, Lamarche-Vane N, and Richard S (2009) An adaptor role for cytoplasmic Sam68 in modulating Src activity during cell polarization. Mol Cell Biol 29, 1933–1943 [PubMed: 19139276]
25. Ramakrishnan P, and Baltimore D (2011) Sam68 is required for both NF-kappaB activation and apoptosis signaling by the TNF receptor. Molecular cell 43, 167–179 [PubMed: 21620750]
26. Fu K, Sun X, Zheng W, Wier EM, Hodgson A, Tran DQ, Richard S, and Wan F (2013) Sam68 modulates the promoter specificity of NF-kappaB and mediates expression of CD25 in activated T cells. Nature communications 4, 1909
27. Zhou J, Zhu Y, Cheng M, Dinesh D, Thorne T, Poh KK, Liu D, Botros C, Tang YL, Reisdorph N, Kishore R, Losordo DW, and Qin G (2009) Regulation of vascular contractility and blood pressure by the E2F2 transcription factor. Circulation 120, 1213–1221 [PubMed: 19752322]
28. Bielli P, Busa R, Di Stasi SM, Munoz MJ, Botti F, Kornblihtt AR, and Sette C (2014) The transcription factor FBI-1 inhibits SAM68-mediated BCL-X alternative splicing and apoptosis. EMBO Rep 15, 419–427 [PubMed: 24514149]
29. Sellier C, Rau F, Liu Y, Tassone F, Hukema RK, Gattoni R, Schneider A, Richard S, Willemsen R, Elliott DJ, Hagerman PJ, and Charlet-Berguerand N (2010) Sam68 sequestration and partial loss of function are associated with splicing alterations in FXTAS patients. EMBO J 29, 1248–1261 [PubMed: 20186122]
30. Li LJ, Zhang FB, Liu SY, Tian YH, Le F, Lou HY, Huang HF, and Jin F (2014) Decreased expression of SAM68 in human testes with spermatogenic defects. Fertil Steril 102, 61–67 e63 [PubMed: 24794312]
31. Paronetto MP, Messina V, Barchi M, Geremia R, Richard S, and Sette C (2011) Sam68 marks the transcriptionally active stages of spermatogenesis and modulates alternative splicing in male germ cells. Nucleic Acids Res 39, 4961–4974 [PubMed: 21355037]
32. Richard S, Torabi N, Franco GV, Tremblay GA, Chen T, Vogel G, Morel M, Cleroux P, Forget-Richard A, Komarova S, Tremblay ML, Li W, Li A, Gao YJ, and Henderson JE (2005) Ablation of the Sam68 RNA binding protein protects mice from age-related bone loss. PLoS genetics 1, e74 [PubMed: 16362077]
33. Zhou J, Cheng M, Boriboun C, Ardehali MM, Jiang C, Liu Q, Han S, Goukassian DA, Tang YL, Zhao TC, Zhao M, Cai L, Richard S, Kishore R, and Qin G (2015) Inhibition of Sam68 triggers adipose tissue browning. The Journal of endocrinology 225, 181–189 [PubMed: 25934704]
34. Huot ME, Vogel G, Zabarauskas A, Ngo CT, Coulombe-Huntington J, Majewski J, and Richard S (2012) The Sam68 STAR RNA-binding protein regulates mTOR alternative splicing during adipogenesis. Molecular cell 46, 187–199 [PubMed: 22424772]
35. Spalding KL, Arner E, Westermark PO, Bernard S, Buchholz BA, Bergmann O, Blomqvist L, Hoffstedt J, Naslund E, Britton T, Concha H, Hassan M, Ryden M, Frisen J, and Arner P (2008) Dynamics of fat cell turnover in humans. Nature 453, 783–787 [PubMed: 18454136]
36. Rigamonti A, Brennand K, Lau F, and Cowan CA (2011) Rapid cellular turnover in adipose tissue. PloS one 6, e17637 [PubMed: 21407813]

37. Townsend KL, and Tseng YH (2014) Brown fat fuel utilization and thermogenesis. Trends in endocrinology and metabolism: TEM 25, 168–177 [PubMed: 24389130]

38. Garg A (2011) Clinical review#: Lipodystrophies: genetic and acquired body fat disorders. J Clin Endocrinol Metab 96, 3313–3325 [PubMed: 21865368]

39. Brown RJ, Araujo-Vilar D, Cheung PT, Dunger D, Garg A, Jack M, Mungai L, Oral EA, Patni N, Rother KI, von Schnurbein J, Sorkina E, Stanley T, Vigouroux C, Wabitsch M, Williams R, and Yorifuji T (2016) The Diagnosis and Management of Lipodystrophy Syndromes: A Multi-Society Practice Guideline. J Clin Endocrinol Metab 101, 4500–4511 [PubMed: 27710244]

40. Wu J, Cohen P, and Spiegelman BM (2013) Adaptive thermogenesis in adipocytes: is beige the new brown? Genes & development 27, 234–250 [PubMed: 23388824]

41. Caron A, Lee S, Elmquist JK, and Gautron L (2018) Leptin and brain-adipose crosstalks. Nat Rev Neurosci 19, 153–165 [PubMed: 29449715]

42. Kooijman S, van den Heuvel JK, and Rensen PCN (2015) Neuronal Control of Brown Fat Activity. Trends in endocrinology and metabolism: TEM 26, 657–668 [PubMed: 26482876]

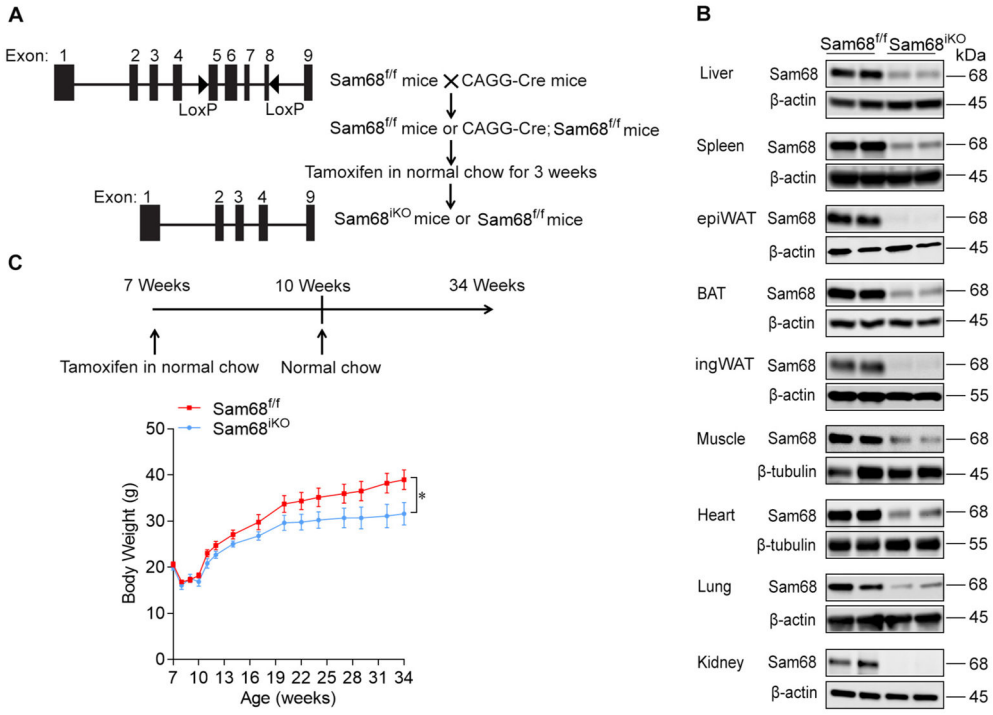

Figure 1. Ablation of Sam68 in adult mice leads to body weight reduction.

(A) *Sam68*$^{f/w}$ mice were generated by homologous recombination, back-crossed to C57BL/6J background for 10 generations, then bred with *CAGG-Cre* mice to generate *CAGG-Cre;Sam68*$^{f/f}$ mice and *Sam68*$^{f/f}$ littermates; induced Sam68 knockout (*Sam68*^{iKO}) mice were obtained by feeding 7 week-old *CAGG-Cre;Sam68*$^{f/f}$ mice with tamoxifen-containing chow for 3 weeks, and similarly treated *Sam68*$^{f/f}$ littermates were controls. **(B)** Western blotting analysis of Sam68 protein expression in the liver, spleen, epididymal white adipose tissue (epiWAT), brown adipose tissue (BAT), inguinal white adipose tissue (ingWAT), skeletal muscle, heart, lung, and kidney of *Sam68*^{iKO} mice and *Sam68*$^{f/f}$ littermates after 3-week tamoxifen treatment. **(C)** Serial measurements of body weights in *Sam68*^{iKO} and *Sam68*$^{f/f}$ mice. n=8-13. Data are expressed as mean ± s.e.m. *p<0.05 (two-way ANOVA).

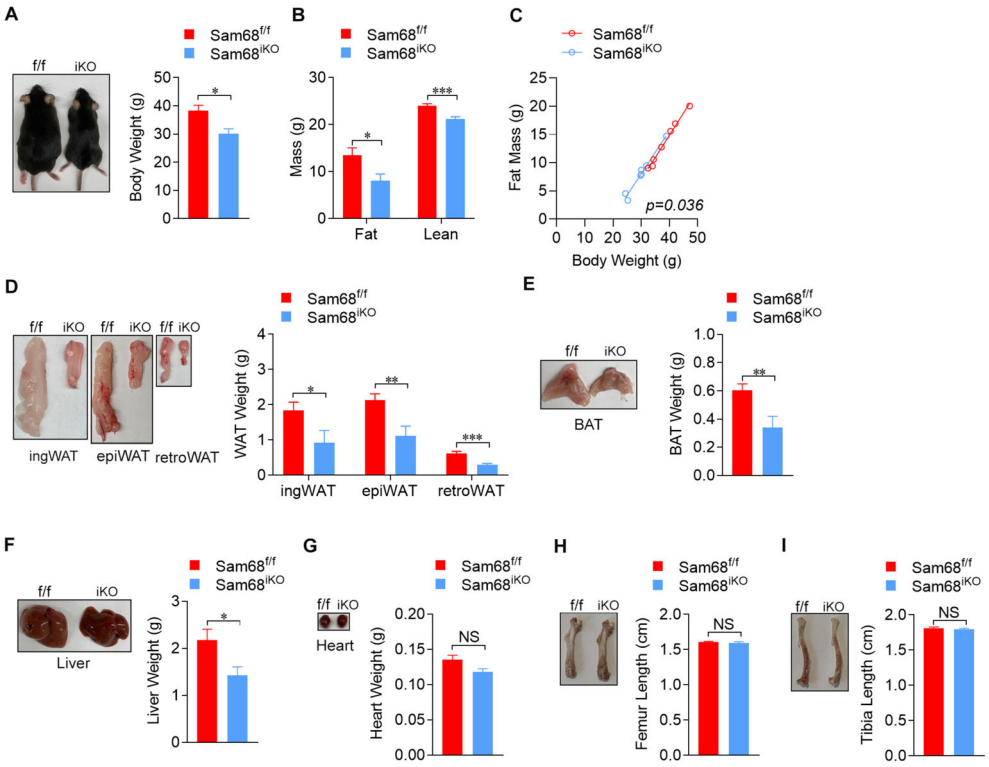

Figure 2. Ablation of Sam68 in adult mice leads to reduced adiposity.

Sam68^{iKO} and Sam68$^{f/f}$ mice were analyzed at 34 weeks old (24 weeks after completion of tamoxifen treatment). **(A)** Gross morphology (*left* panel) and body weight measurements (*right* panel). **(B)** Body compositions (fat mass and lean mass) were assessed by quantitative magnetic resonance (QMR). **(C)** Relationship between fat mass and body weight. **(D-G)** Gross morphology (*left* panel) and weight measurements (*right* panel) of **(D)** epiWAT, ingWAT, retroperitoneal white adipose tissue (retroWAT), **(E)** brown adipose tissue (BAT), **(F)** liver and **(G)** heart. (**H-I**) Gross morphology (*left* panel) and length measurements (*right* panel) of the femur **(H)** and tibia **(I)**. n=7-11 per group. Data are expressed as mean ± s.e.m. *p<0.05, **p<0.01, ***p<0.001, NS, not significant. (A-B and D-I: unpaired two-tailed *t* test; C: ANCOVA).

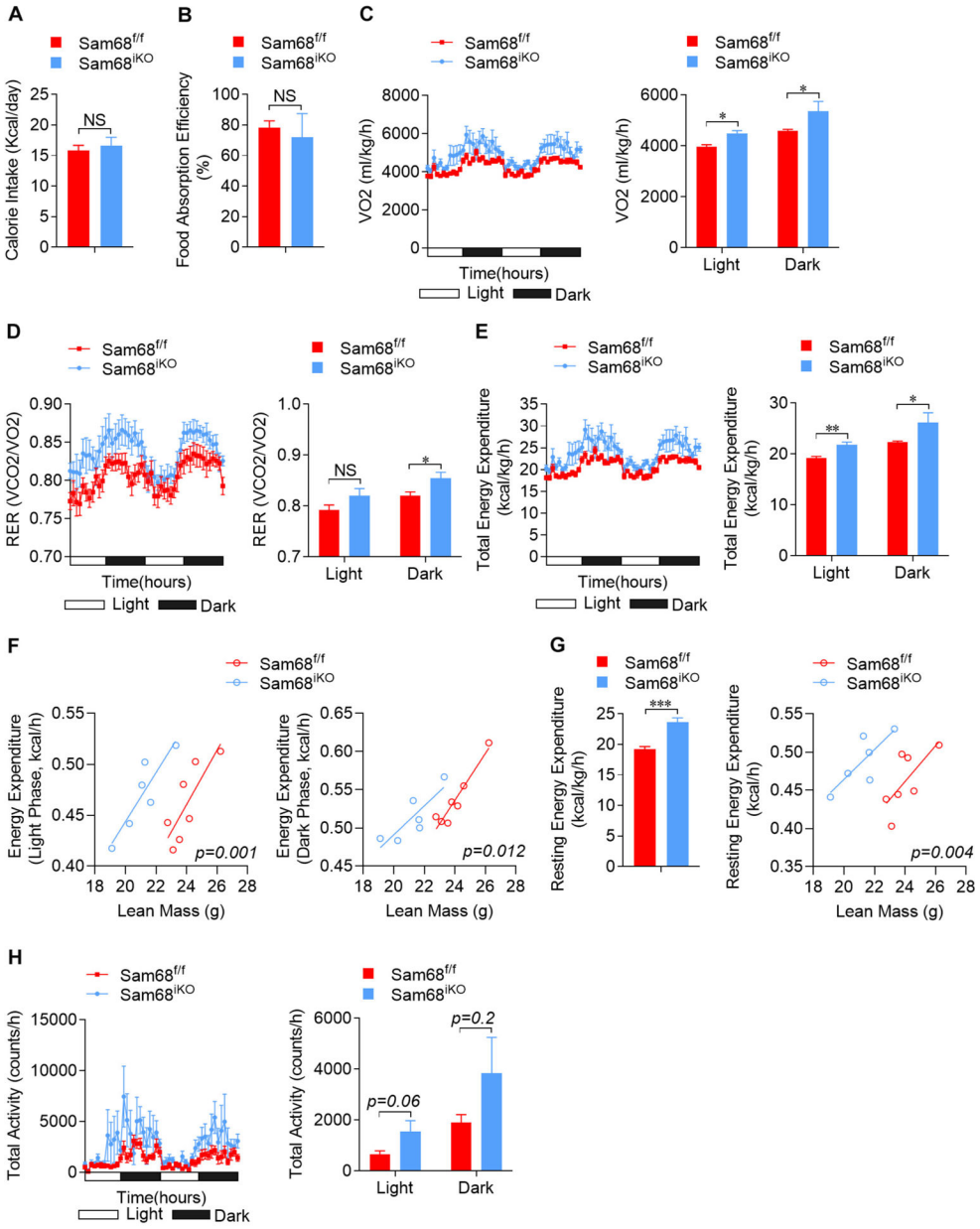

Figure 3. Ablation of Sam68 in adult mice leads to increased energy expenditure.

Sam68^{iKO} mice and Sam68$^{f/f}$ littermates at 34 weeks old were analyzed. **(A)** Food intakes were measured by indirect calorimetry system. **(B)** Food absorption efficiency were assessed by bomb calorimeter. **(C-H)** Indirect calorimetry assessments of **(C)** oxygen consumption (VO2), **(D)** respiratory exchange ratio (RER), **(E)** total energy expenditure, (**F**) relationship of energy expenditure and lean mass at light (*left* panel) and dark (*right* panel) phases, **(G)** resting energy expenditure (*left* panel) and relationship of resting energy expenditure and lean mass (*right* panel), and **(H)** locomotor activity. n=6-7 per group. Data are expressed as mean ± s.e.m. *p<0.05, **p<0.01 (A-B and *left* panel of G: unpaired two-tailed *t* test; C-E and H: two-way ANOVA; F and *right* panel of G: ANCOVA).

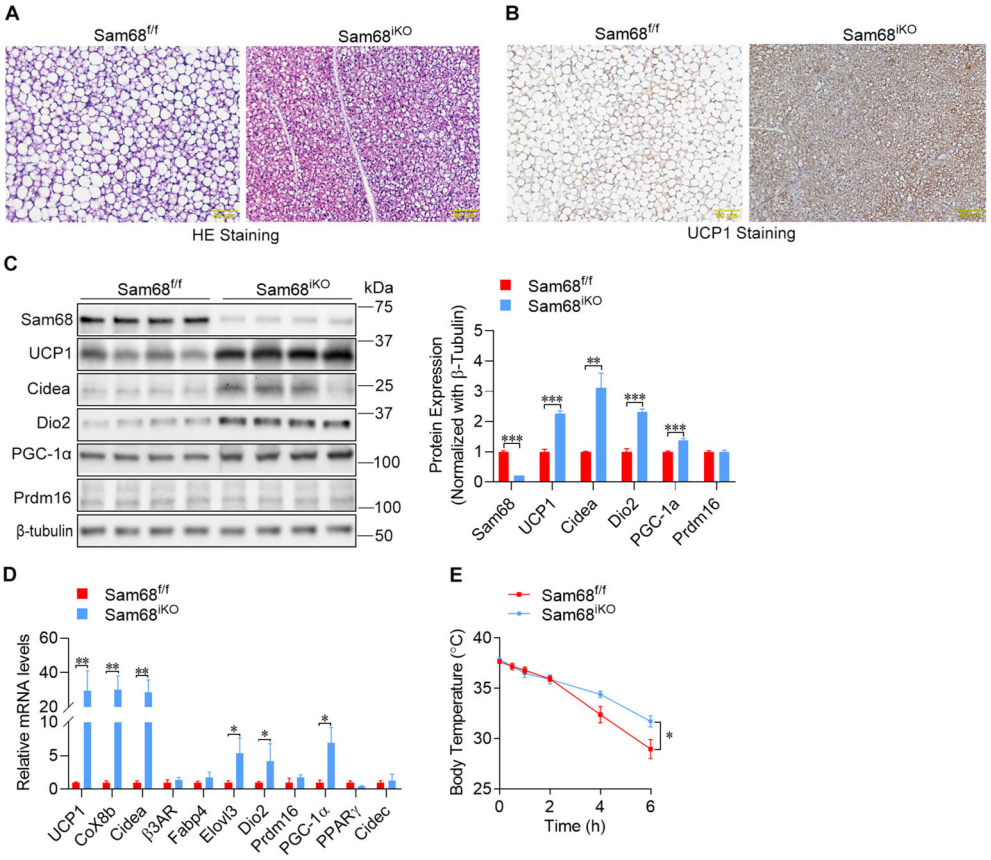

Figure 4. Ablation of Sam68 in adult mice leads to increased thermogenesis in BAT.

(A-D) BAT was isolated from 36-week-old Sam68^{iKO} mice and Sam68$^{f/f}$ littermates. **(A)** H&E staining of paraffin-embedded sections. Scale bar = 50 μM. **(B)** Immunohistochemical staining of UCP1 protein. Scale bar = 50 μM. **(C)** Representative Western blotting (*left* panel) and quantification (*right* panel) of protein levels of Sam68 and thermogenic markers. **(D)** mRNA levels of genes involved in thermogenesis and fatty acid oxidation were quantified by qRT-PCR and normalized to that of β-actin. **(E)** Rectal body temperature measurements in 36-week-old Sam68^{iKO} and Sam68$^{f/f}$ mice after cold (4°C) exposure for 0 (basal), 30 min, 1, 2, 4, and 6 h. n=7-8 per group. Data are expressed as mean ± s.e.m. *p<0.05, **p<0.01, ***p<0.001 (*right* panel of C and D: unpaired two-tailed *t* test; E: two-way ANOVA).

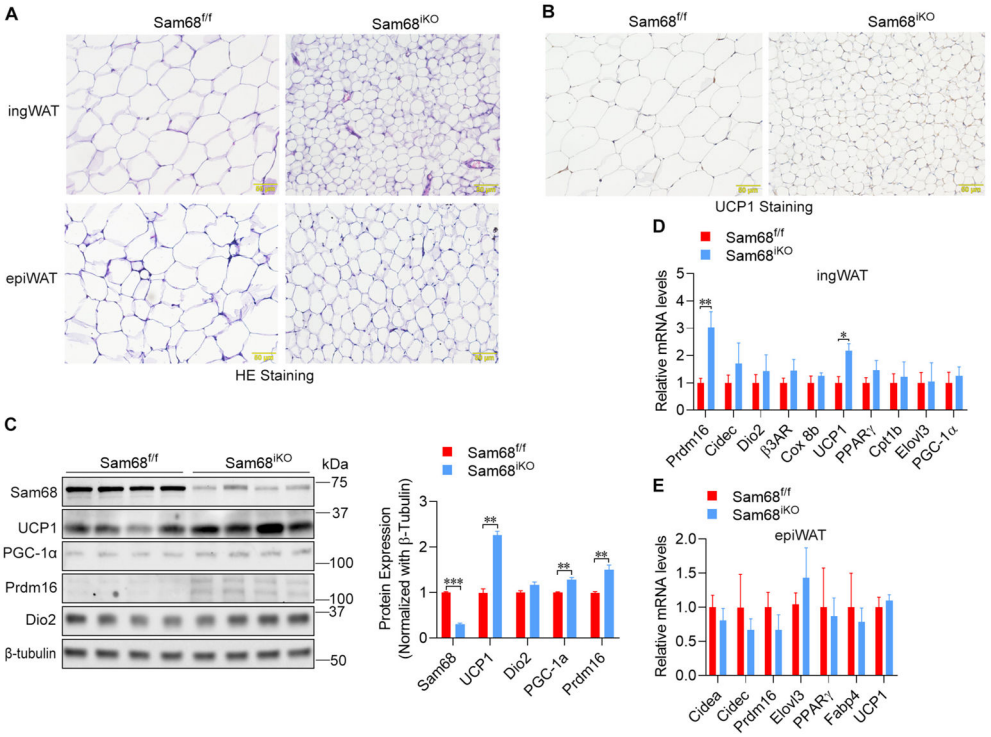

Figure 5. Ablation of Sam68 in adult mice enhances the browning signature of WAT.

Inguinal and epididymal WATs were isolated from 36-week-old Sam68^{iKO} mice and Sam68$^{f/f}$ littermates. **(A-B)** H&E staining **(A)** and immunohistochemical detection of UCP1 protein expression **(B)** in paraffin-embedded WAT sections. Scale bar = 50 μM. **(C)** Representative Western blotting (*left* panel) and quantification (*right* panel) of protein expression of UCP1 and thermogenic genes in ingWAT. **(D-E)** qRT-PCR quantification of mRNA expression of thermogenesis and fatty acid oxidation genes in ingWAT **(D)** and epiWAT **(E)**, respectively. mRNA expression was normalized to the level of β-actin. n=7-8 per group. Data are expressed as mean ± s.e.m. *p<0.05, **p<0.01, ***p<0.001 (unpaired two-tailed *t* test).

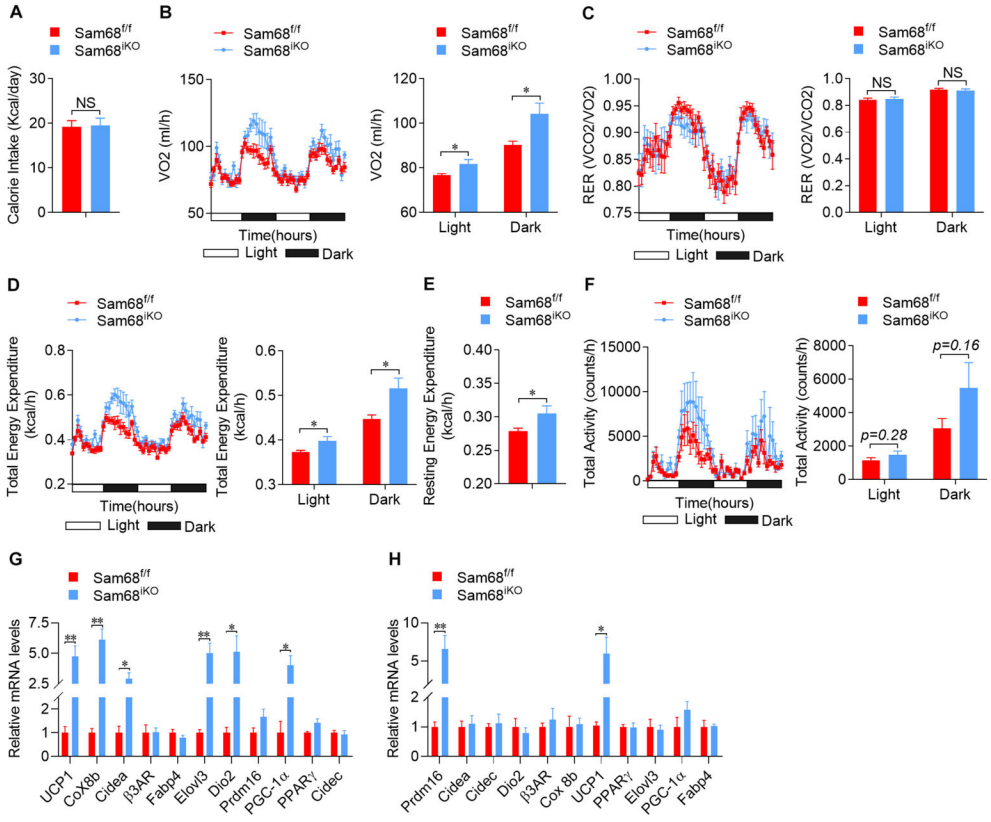

Figure 6. Ablation of Sam68 in adult mice leads to increased energy expenditure and thermogenic gene expression before their body weights deviate.

Eleven week-old Sam68^{iKO} mice and Sam68$^{f/f}$ littermates (one week after completion of tamoxifen treatment) were analyzed. **(A-F)** Indirect calorimetry analysis of **(A)** daily calorie intake, **(B)** oxygen consumption (VO2), **(C)** respiratory exchange ratio (RER), **(D)** total energy expenditure, **(E)** resting energy expenditure, and **(F)** locomotor activity. n=7 per group. **(G-H)** qRT-PCR analysis of mRNA expression of thermogenesis and fatty-acid oxidation genes in **(G)** BAT and **(H)** ingWAT, respectively. n=4 per group. Data are expressed as mean ± s.e.m. *p<0.05, **p<0.01 (A, E, and G-H: unpaired two-tailed *t* test; B-D and F: two-way ANOVA).